Presentation at JAXA to JHS members

Recent Activities on Rotorcraft CFD at Konkuk University

Soo Hyung Park

Department of Mechanical and Aerospace Engineering,
Konkuk university

February 19, 2023

Contents

- Introduction to KFLOW Solver

- Application to Helicopter Aerodynamics
  - Propeller-Wing Interaction
  - HART-II
  - Co-axial Rotor
  - Passive/Active Fuselage Drag Reduction

URANS SOLVER (KFLOW) INTRODUCTION

Helicopter Aerodynamics

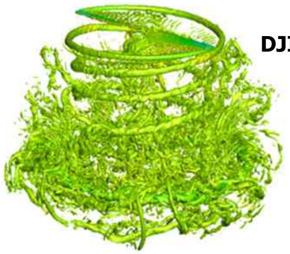
DJI 9450 Propeller

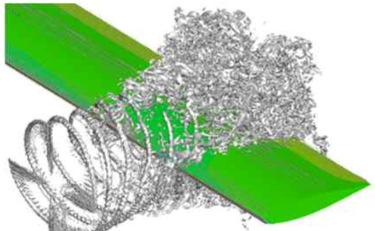
Propeller-Wing

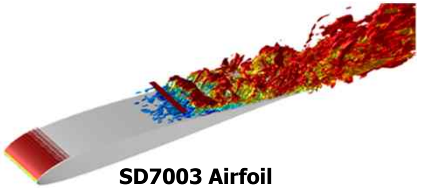
SD7003 Airfoil
(Laminar-turbulent transition)

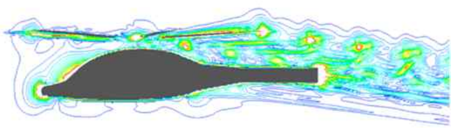
LCH Helicopter (KAI)


Co-rotating stacked rotor

KFLOW

- Parallelized Structured Compressible Navier-Stokes Equations
- Low-Mach number Preconditioning
- Thermo-Chemical nonequilibrium reactive flows
- Chimera Overset Grid System
- 6-DOF Simulations for multiple moving bodies
- Flux / Time schemes
  - ✓ Flux: Roe's FDS / HLLE+ / AUSMPW+ / M-AUSMPW+
  - ✓ Interpolations: TVD MUSCL types / WENO-types / eMLP-types
  - ✓ Time: Explicit Runge-Kutta / Implicit (BDF2) with DADI / D-Implicit RK
- Turbulence / Transition Models
  - ✓ Turbulence: SA-types / k-ϵ / k-ω types / DES, DDES / ILES / Roughness
  - ✓ Large Eddy Simulation with Dynamic Smagorinsky subgrid model
  - ✓ Transition: $\gamma - Re_\theta$

Brief Review of eMLP

- Spatial Discretization Methods

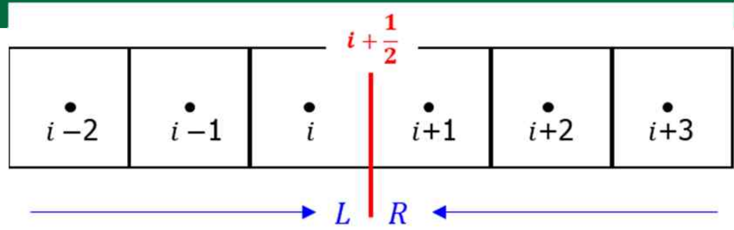

$$\frac{\partial Q}{\partial t}+\frac{\partial F}{\partial x}+\frac{\partial G}{\partial y}+\frac{\partial H}{\partial z}=\frac{\partial F_v}{\partial x}+\frac{\partial G_v}{\partial y}+\frac{\partial H_v}{\partial z}$$

RECONSTRUCTION

$$\frac{(F)_{i+\frac{1}{2}}-(F)_{i-\frac{1}{2}}}{\Delta x}$$

$$F_{i+\frac{1}{2}}=\frac{F_{Left}+F_{Right}}{2}+Numerical\ Dissipation$$

Total Variation Diminishing	Multi-dimensional Limiting Process	Weighted ENO
$\mathrm{TV(u)}=\int\left\lvert\frac{\partial u}{\partial x}\right\rvert dx \leftrightarrow \mathrm{TV}(u^n)$ $=\sum_{i=-\infty}^{+\infty}\lvert u_{i+1}^n-u_i^n\rvert = 2(\sum Maxima - \sum Minima)$ Total Variation Diminishing : $\mathbf{TV}(\boldsymbol{u}^{n+1})\le\mathbf{TV}(\boldsymbol{u}^{n})$ $\boldsymbol{\Phi_L=\bar{\Phi}_i+0.5\phi(r_L)(\bar{\Phi}_i-\bar{\Phi}_{i-1})}$ $\phi_{TVD}(r)=\max(0,\min(2,2r,\beta))$	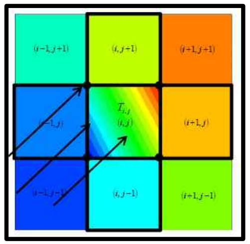 Local Maxima and minima occur in cell vertex ∴ **Cell Vertex Value should be limited.** $\boldsymbol{\Phi_L=\bar{\Phi}_i+0.5\phi(r_L)(\bar{\Phi}_i-\bar{\Phi}_{i-1})}$ $\phi_{MLP}(r)=\max(0,\min(\alpha,\alpha r,\beta))$	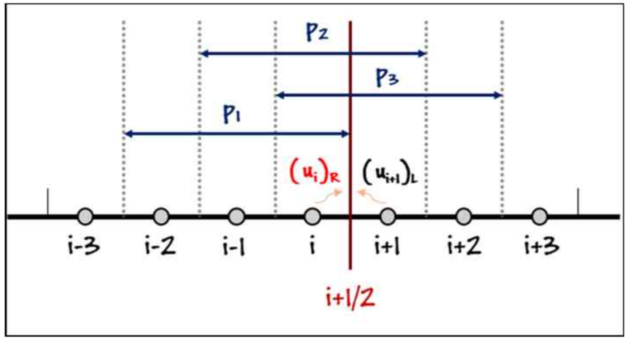 $\boldsymbol{\Phi_L=w_1p_1+w_2p_2+w_3p_3}$

- Strategy : Mixed high-order reconstruction to reduce unnecessary numerical dissipation

eMLP-VC (Newly Modified eMLP)

eMLP-VC (Vorticity Conservation)

- eMLP has been generally developed for a wide variety of flows (including magnetohydrodynamic), the **accuracy for rotorcraft flowfields** can be further improved.
- The **robustness** of eMLP can be refined by maintaining the consistency of the sensing function and the interpolation method.

Rotorcraft flowfields

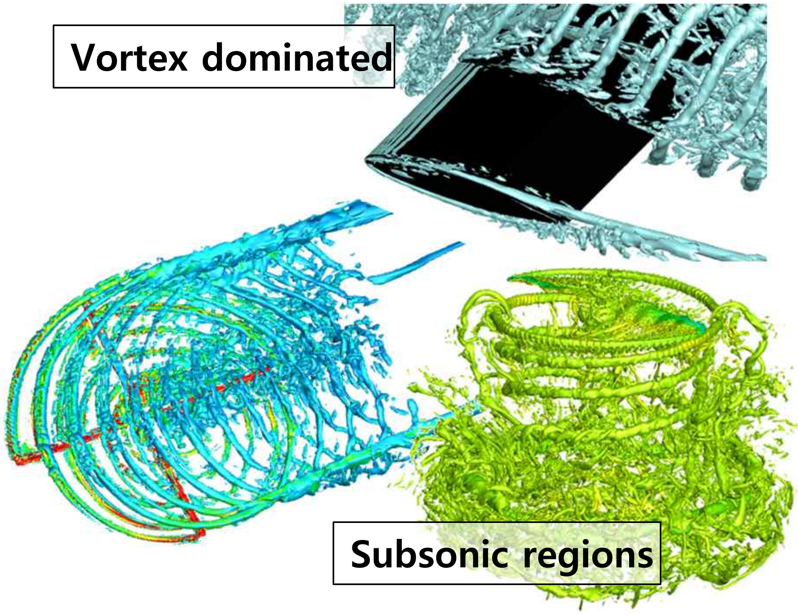

Robustness problem

$$\Phi_{i,approximate} = \frac{-\Phi_{i-2} + 4\Phi_{i-1} + 4\Phi_{i+1} - \Phi_{i+2}}{6}$$

Original sensing function (4th order central differencing)

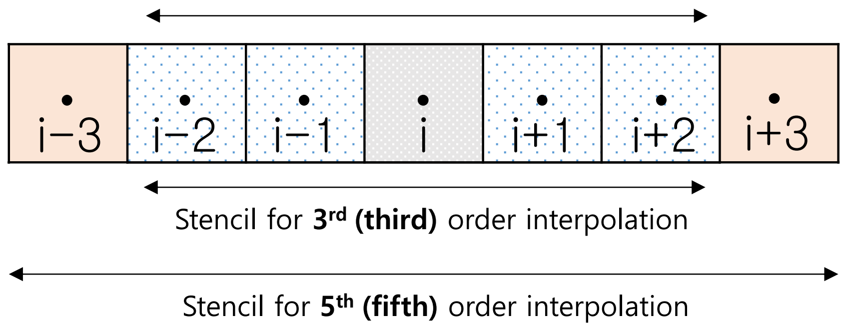

eMLP-VC (Newly Modified eMLP)

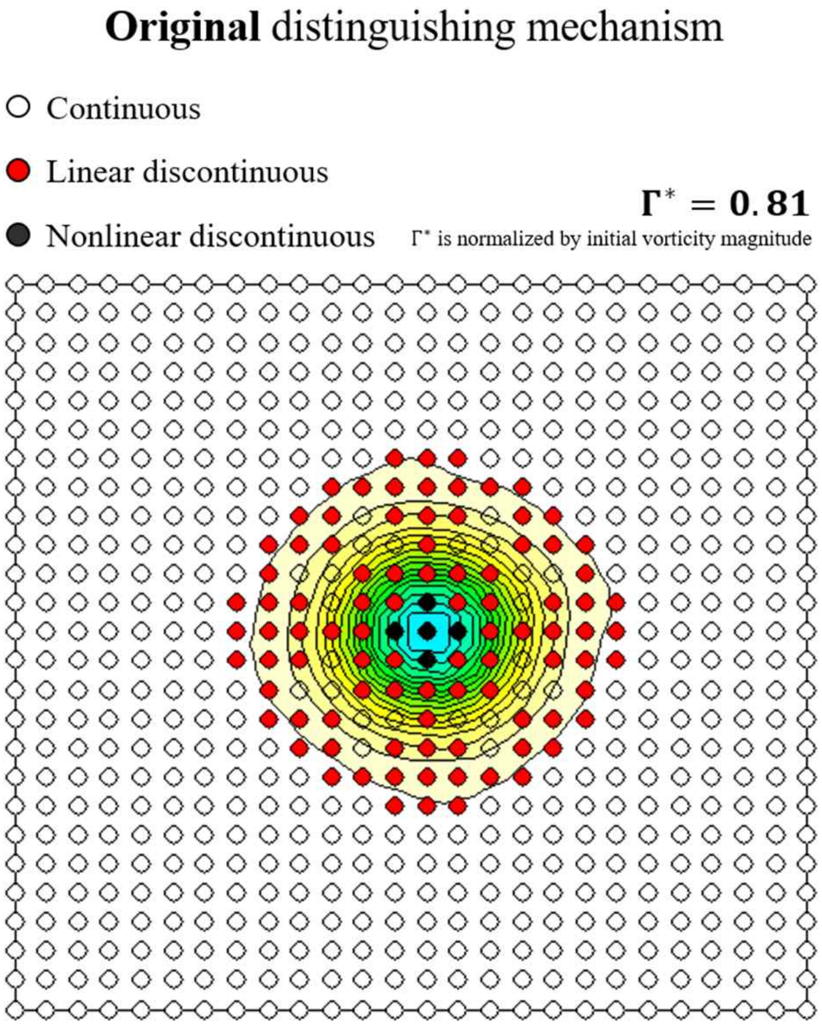

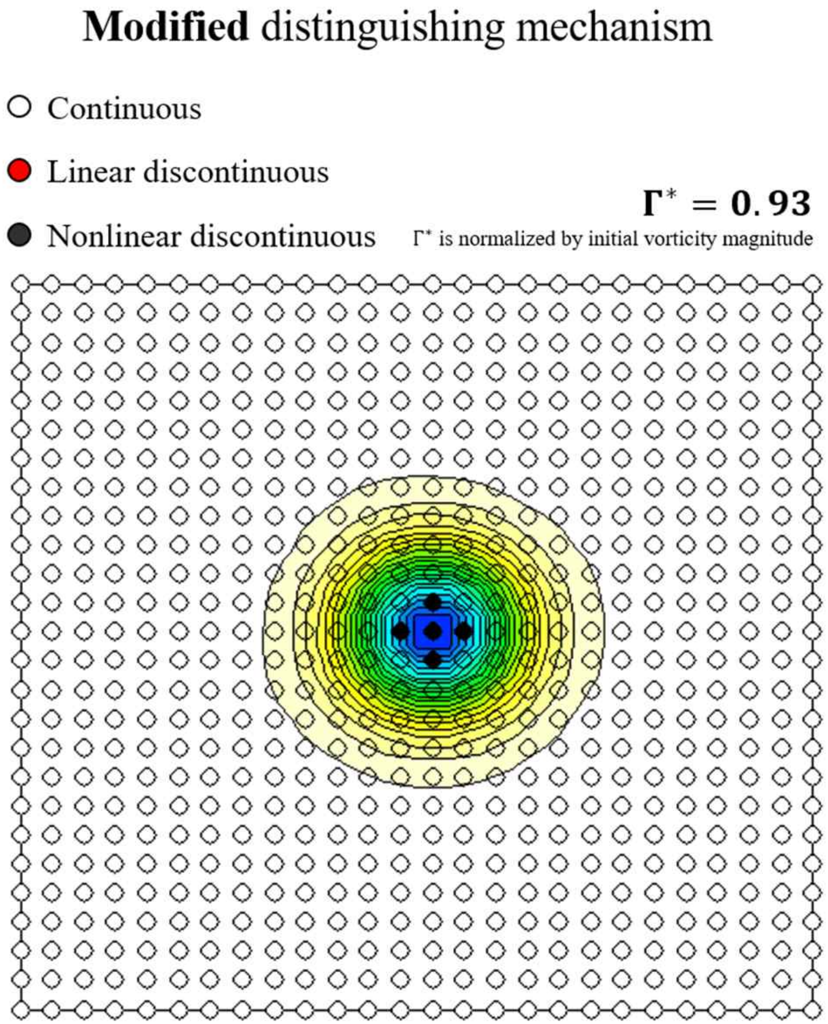

eMLP-VC (Newly Modified eMLP)

Accuracy Improvement of eMLP-VC

- Nonlinear wave propagation (Isentropic vortex)

	No limiter (fifth-order reconstruction)	MLP	eMLP	eMLP-VC
Coarse Grids 5 grids in vortex core Overall domain - 25 × 25 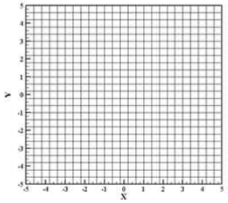	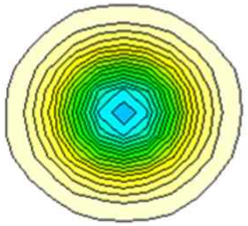 $\Gamma^* = 0.889$	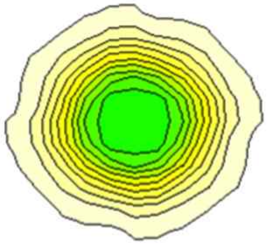 $\Gamma^* = 0.175$	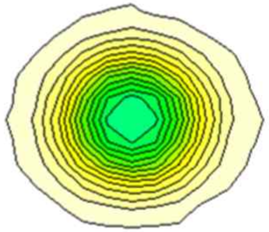 $\Gamma^* = 0.653$	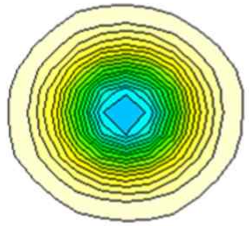 $\Gamma^* = 0.900$
Fine Grids 10 grids in vortex core Overall domain - 50 × 50 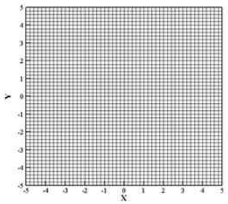	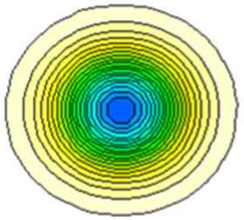 $\Gamma^* = 0.996$	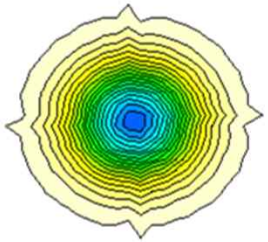 $\Gamma^* = 0.501$	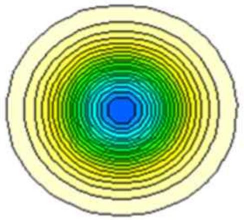 $\Gamma^* = 0.996$	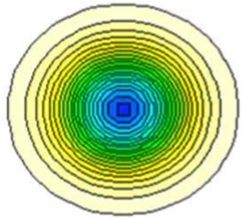 $\Gamma^* = 0.999$

Γ^* is the vorticity magnitude normalized by the initial vorticity magnitude

Application: PROWIM

Propeller – Wing Interaction (PROWIM)

- Tested at TU delft (2005) for analysis of the propeller-wing interaction
- Experiment setting
  - ✓ Wing: rectangular shape with AR 5.33, NACA 64-2-015A airfoil
  - ✓ Propeller: NACA 5868-9, Clark Y airfoil
    Pitch : 25° at 0.75R
  - ✓ Wing incident angle: 4°
  - ✓ Freestream M = 0.14, Re = 0.8×10^{6}
- Solver Information
  - ✓ Temporal Integration : Unsteady (BDF2 with dual time stepping), 1°
  - ✓ Turbulence model : $k-\omega\ Wilcox - Durbin +$
  - ✓ Grids: Blade – O-type, 241×165×81 / y+=1 at tip
    Background : 48,000,000 / 10% chord

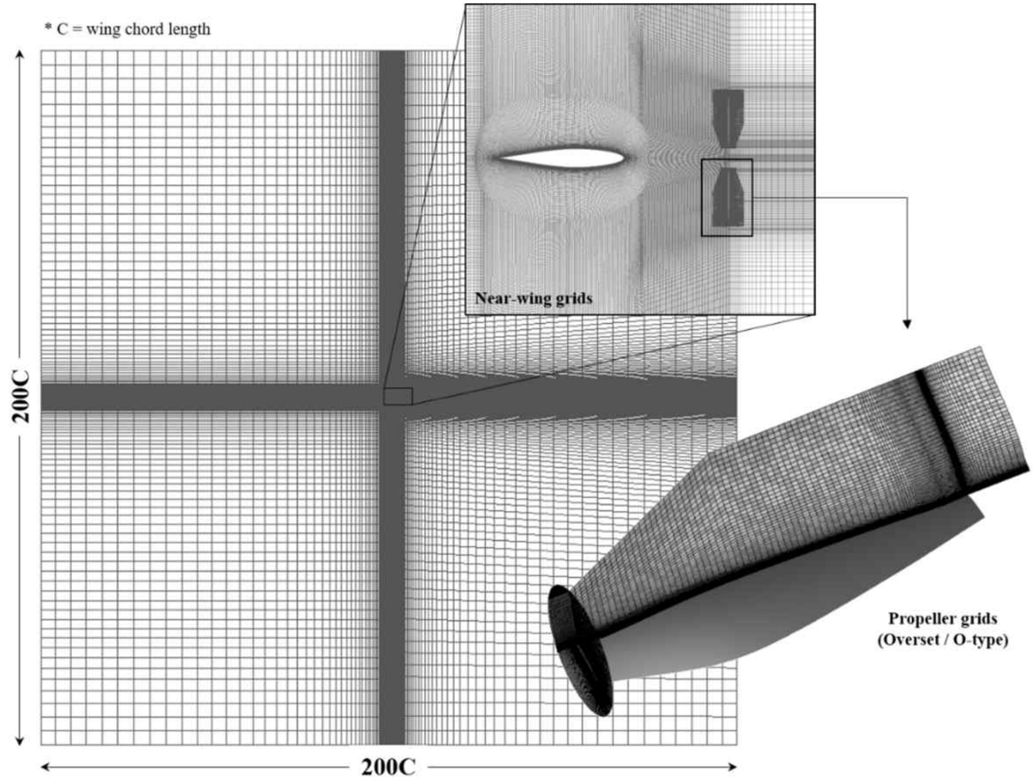

Application: PROWIM

- Propeller – Wing Interaction (PROWIM)

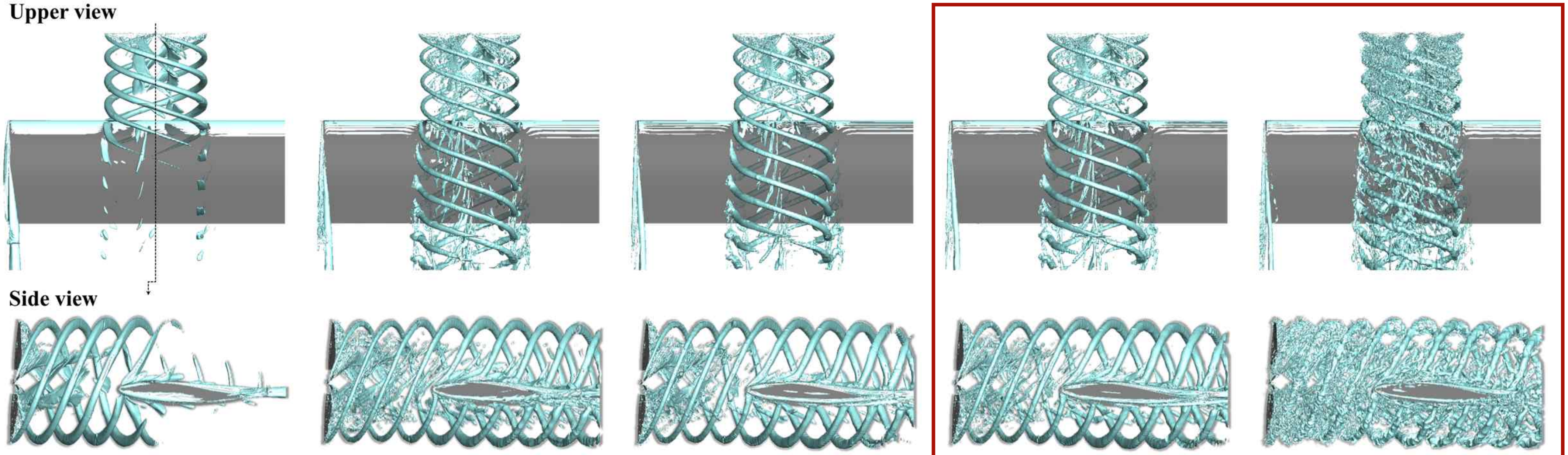

(a) TVD MUSCL limiter (b) WENO (c) MLP (d) eMLP (e) eMLP-VC

Application: PROWIM

- Propeller – Wing Interaction (PROWIM)

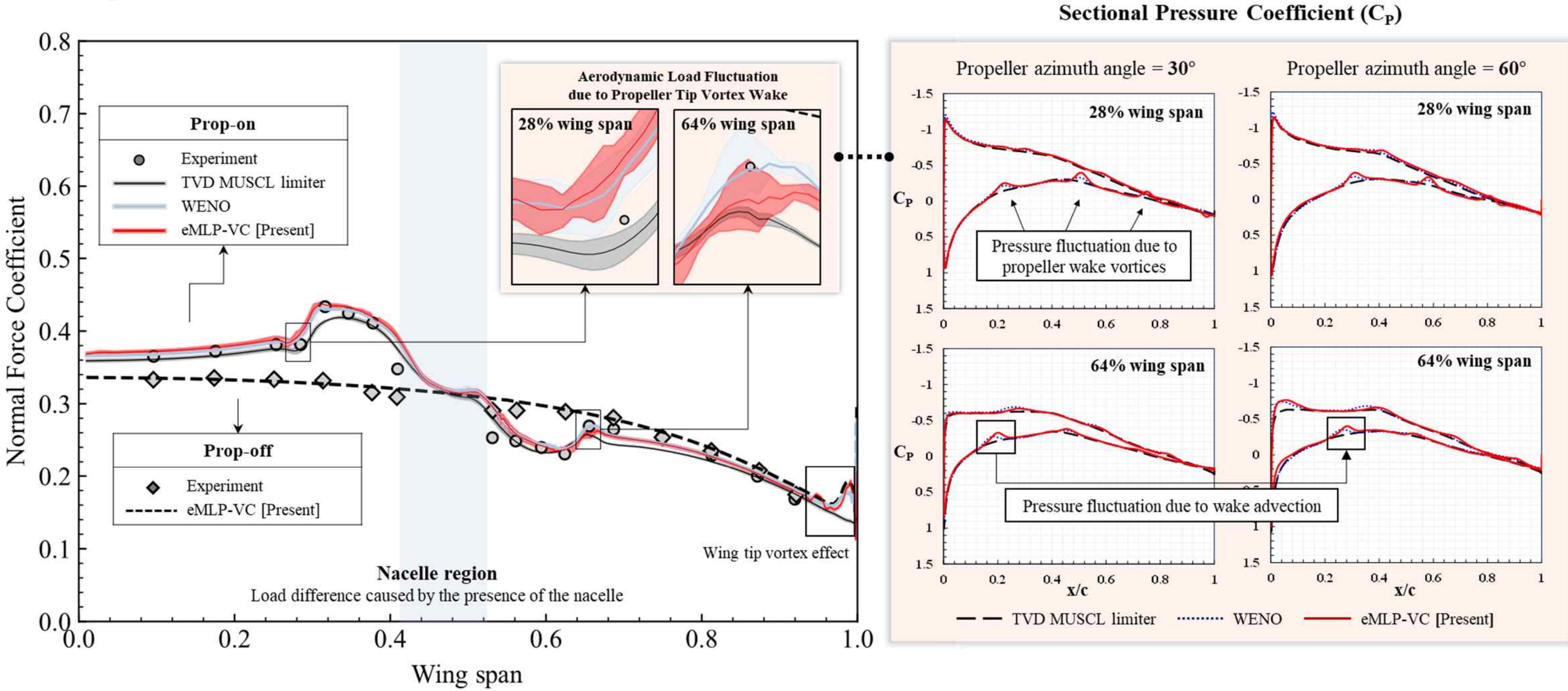

Application: HART-II

- HART II (Second Higher harmonic control Aeroacoustics Rotor Test) case

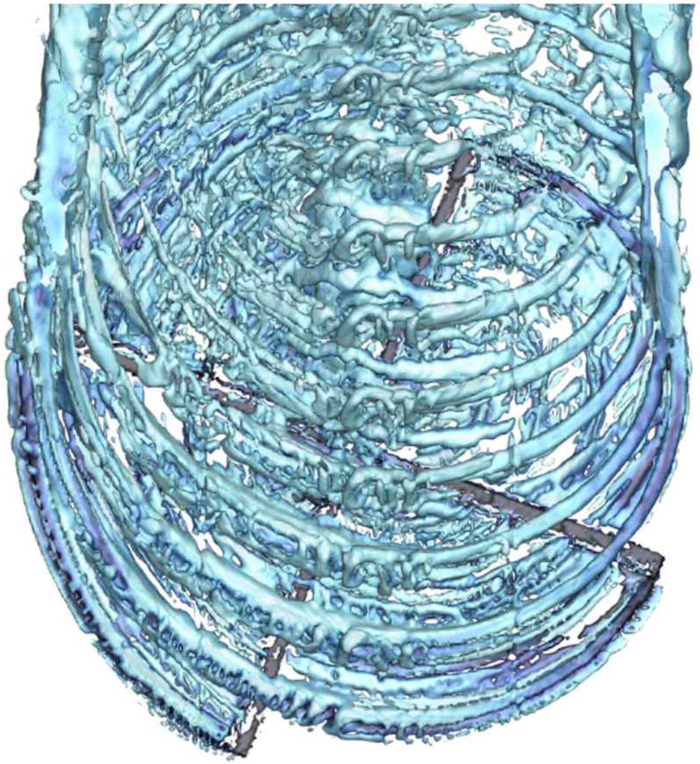

- 2001. German-Dutch wind tunnel (DNW)

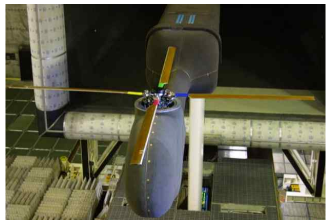

- Representative rotorcraft experiment
- Descent flight condition

  $\mu = 0.15,\ \alpha_{Shaft} = 4.5°$

  Blade-vortex interaction (BVI) dominant flowfield

- Rotor property (BO105 – Mach-scaled blade)

  No. of blades: 4 / Airfoil: NACA23012mod

  Radius: 2m / Chord: 0.121m

Application: HART-II

■ HART II (Second Higher harmonic control Aeroacoustics Rotor Test) case

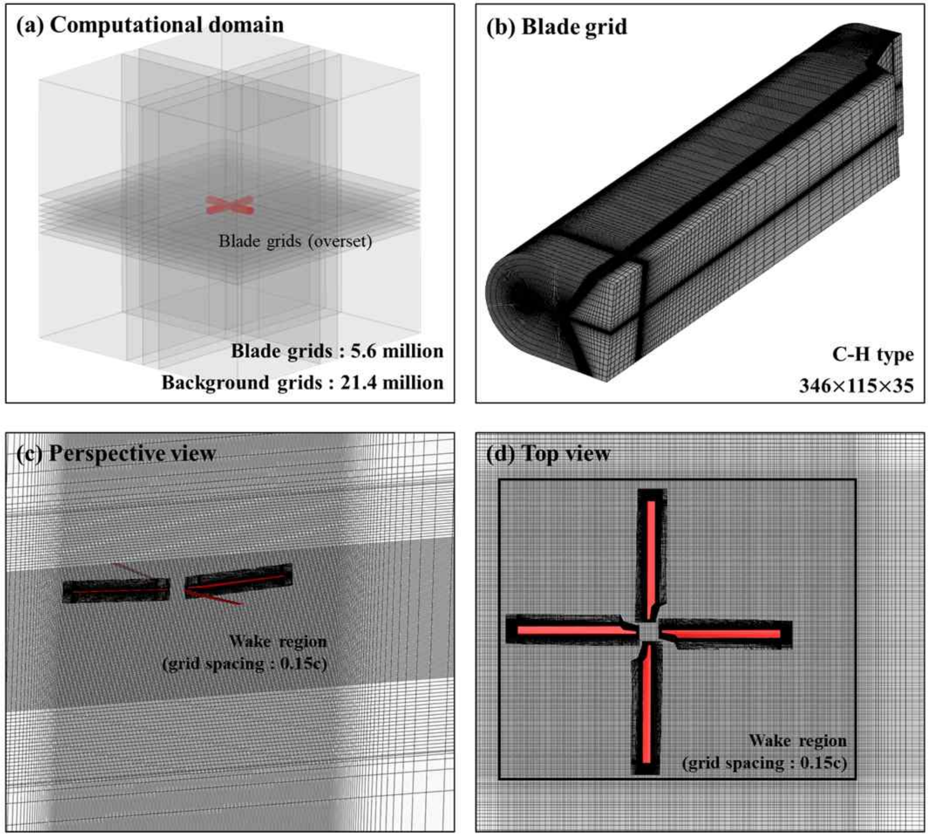

- CFD-CSD loose coupling / Acoustic Analogy
  - ✓ **[Fluid Dynamics] KFLOW**
    - Spatial Discretization: upwind flux function (AUSMPW+)
    - WENO-JS, WENO-M, WENO-Z, eMLP, eMLP-VC
    - Temporal Integration: BDF2 with dual time stepping / Diagonalized ADI
    - Turbulent Equation: $k-\omega$ Wilcox-Durbin+ model
    - Grids : **background: 21M (Minimum $\Delta s = 0.15c$)**
    - **blade: 1.3M (X 4 blades)**
    - **total 26.2M**
  - ✓ **[Structure] CAMRAD II (NASA, Dr. Wayne Johnson)**
    - Structural solver : Beam model (Isotropic with elastic axis / 15 DOF)
    - Aerodynamic solver : Free wake with static stall model / Rigid wake model
  - ✓ **[Aeroacoustic] KR-NOISE (KARI, Dr. Wie Sung Yong)**
    - Ffocs-Williams and Hawkings eqn.
    - Loading noise & Thickness noise

Application: HART-II

- Results of HART II

Normal force distribution (at r/R=0.87)

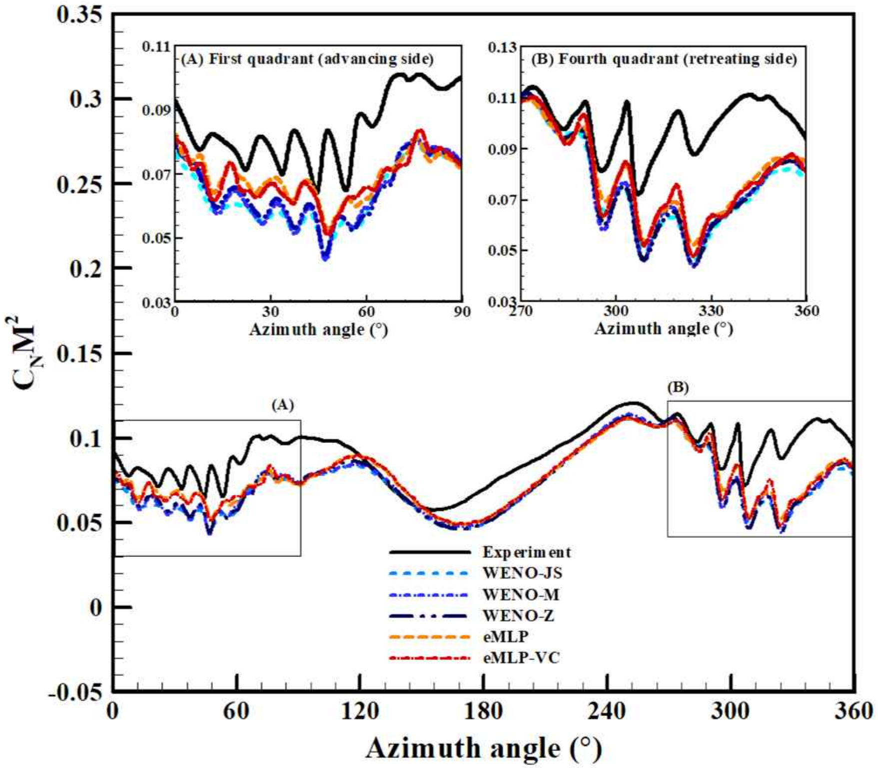

Derivative of normal force (at r/R=0.87)

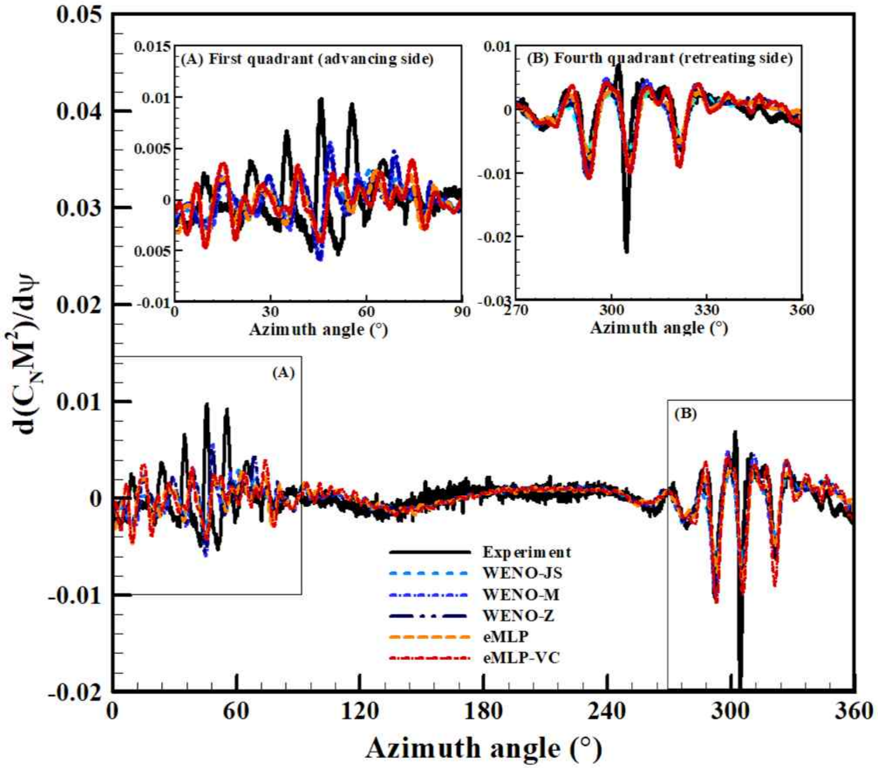

Application: HART-II

- Tonal noise comparison (using Farassat 1A eqn. / KR-noise)
  - Mid-frequency noise (Blade pass frequency of 6 to 40)
  - Mic → -2.2m (1 Radius)

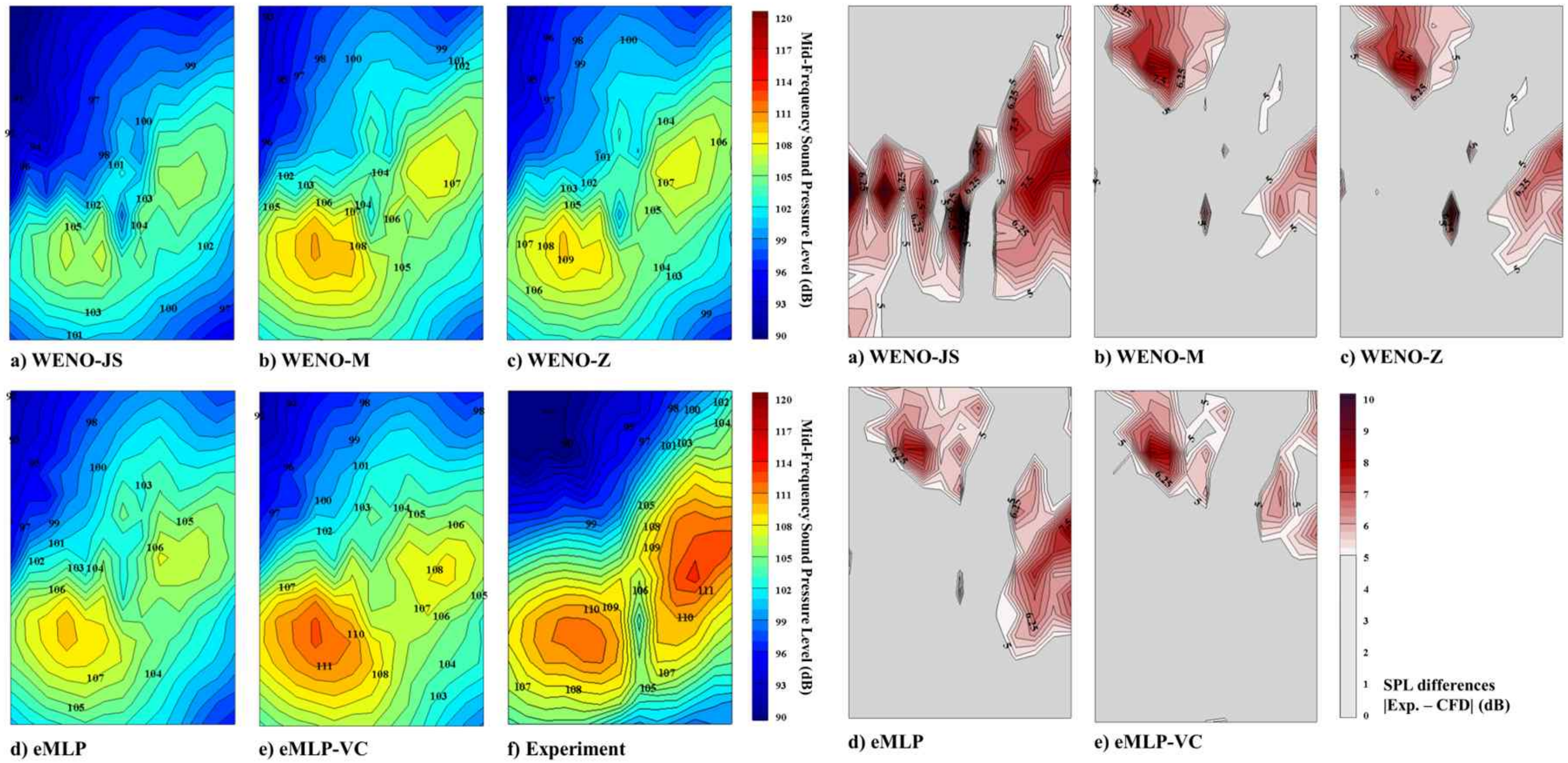

Application: Stacked Rotor

- Co-rotating coaxial rotor ('=stacked rotor')
  - Also called as 'stacked rotor'

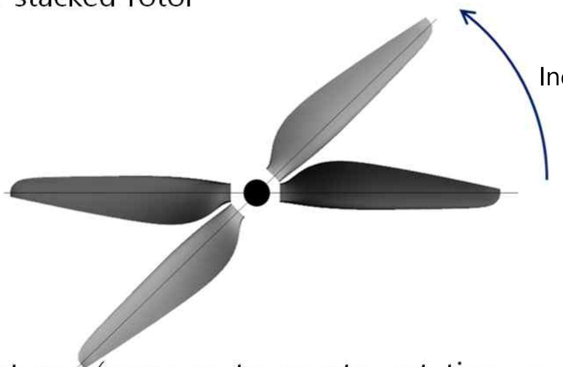

  - Possible advantages (compare to counter-rotating coaxial rotor)
    - ✓ No need to consider the "torque balance"
      - Optimized pitch angle (upper / lower rotor both)
        → **Gain in aerodynamic performance (efficiency)**
    - ✓ Can avoid Blade/vortex interaction (BVI) condition
      - Counter-rotating rotor always have BVI in 1 rev.
        Co-rotating rotor can avoid the BVI (optimizing the index angle)
        → **Reduction of noise / vibration**
  - Several researches have been conducted for UAM/UAV aircraft
  - Analyzed by Prof. K. Yee and Dr. Y.P. Hong (SNU) with KFLOW

Quantification of Swirl Recovery in a Coaxial Rotor System
2017, American Helicopter Society Annual Forum, Corresponding author: Daiju Uehara, Jayant Sirohi (Univ. of Texas)

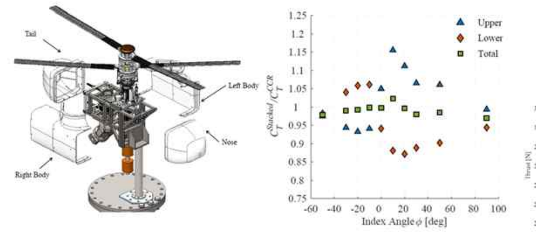

Rotor system	η_u	η_l	$\eta_{stacked/CCR}$
CCR	1.220	1.396	N/A
Stacked at $\phi = 90°$	1.223	1.503	1.040
at $\phi = 10°$	0.982	1.668	0.960
at $\phi = 0°$	1.134	1.510	0.996
at $\phi = -10°$	1.337	1.285	0.995
at $\phi = -50°$	1.267	1.416	1.027

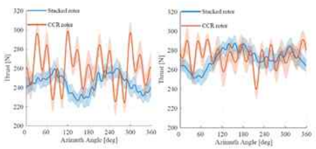

Experimental and computational investigation of stacked rotor performance in hover
2021, Aerospace Science and Technology, George Jacobellis, Rajneesh Singh, Chloe Johnson, Jayant Sirohi, Rob McDonald

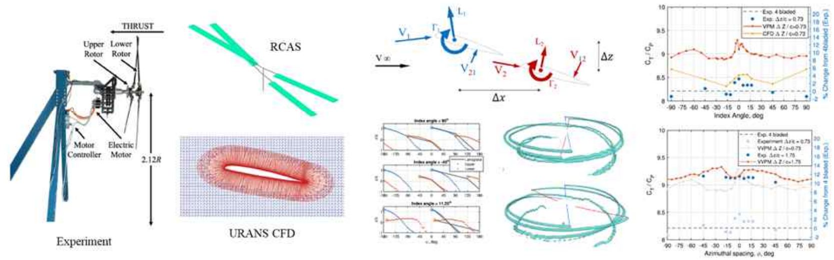

Wake of a Coaxial Corotating Rotor in Hover
2022, AIAA Journal, John Valdez, Charles E. Tinney (University of Texas at Austin)

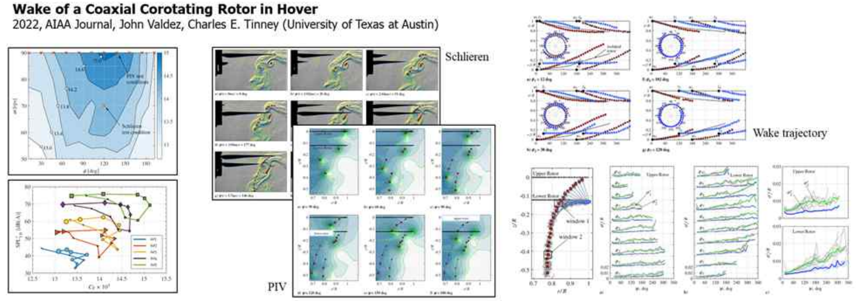

Application: Stacked Rotor

- Flowfields of DOE cases (snapshot of each cases)
  - Vortex field visualized by iso-surface method using Q-criterion

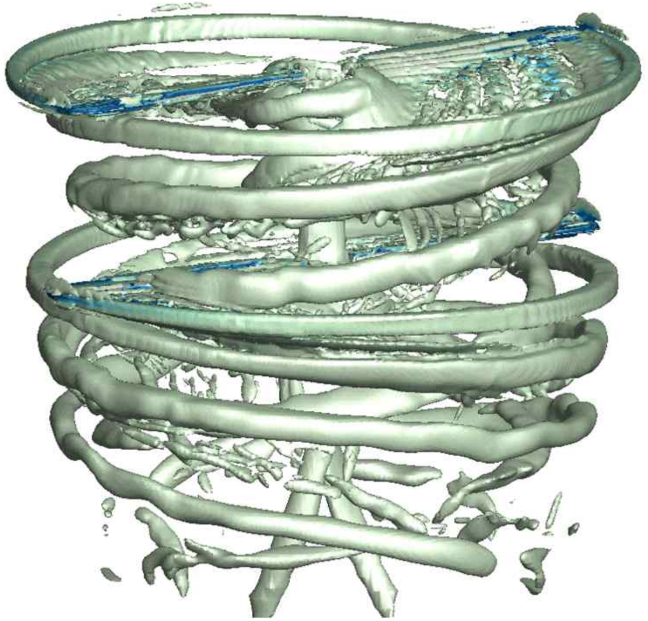

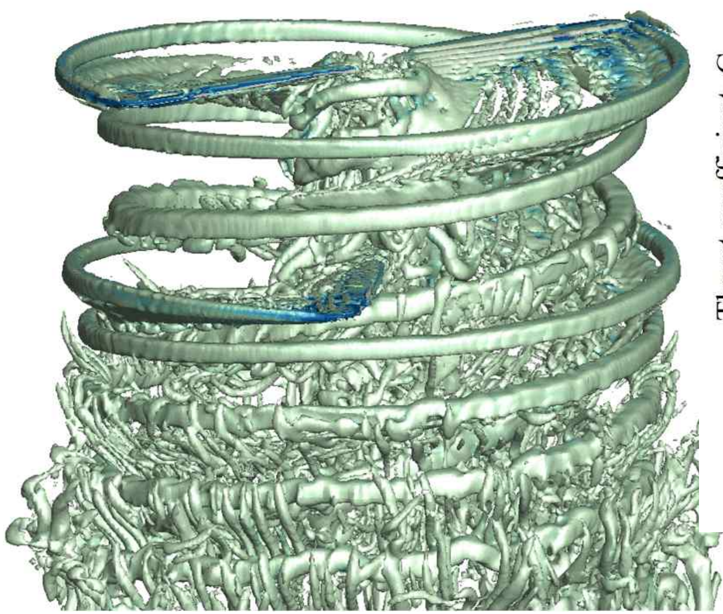

Thrust history

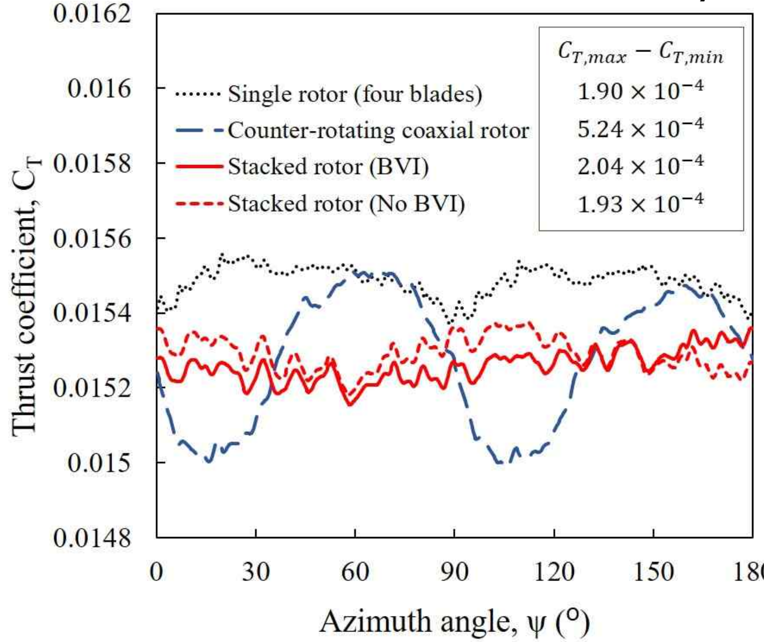

Stacked rotor with BVI ($Z = 0.3D, \phi = 45°$, $\Delta\theta = 0°$)

Counter-rotating coaxial rotor ($Z = 0.3D$, $\Delta\theta = trimmed$)

Passive Reduction of Fuselage Drag

- Subsonic Wind Tunnel

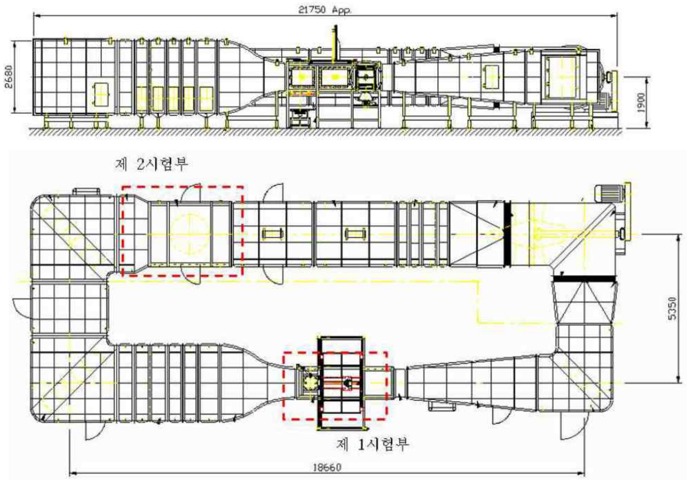

- Internal Balance (KB-40)
  - 6-Component Internal Balance (5 forces, 1 moment)
  - Strain Gauge Type
  - Calibration Process with Multiple Linear Regression

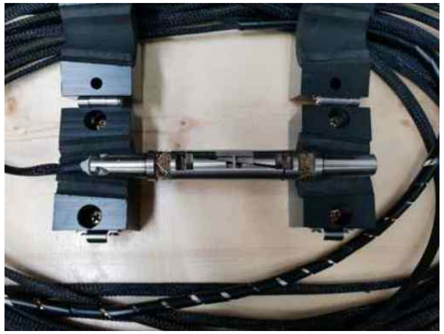

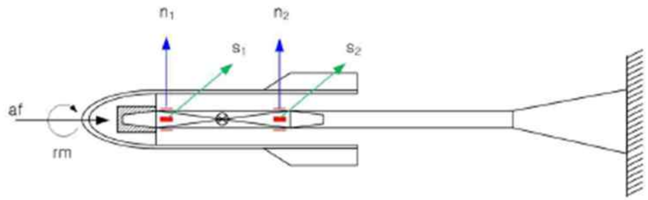

- High-speed Compound Rotorcraft

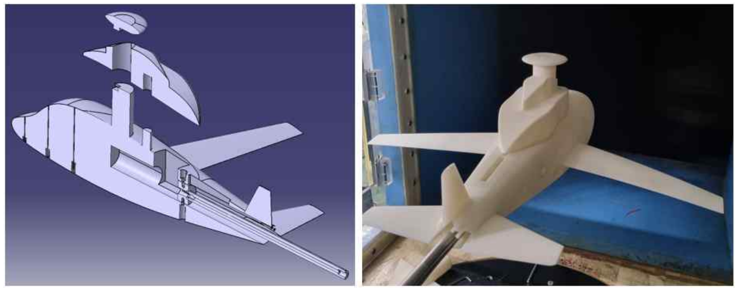

<Manufacturing Scale-down Model>

Passive Reduction of Fuselage Drag

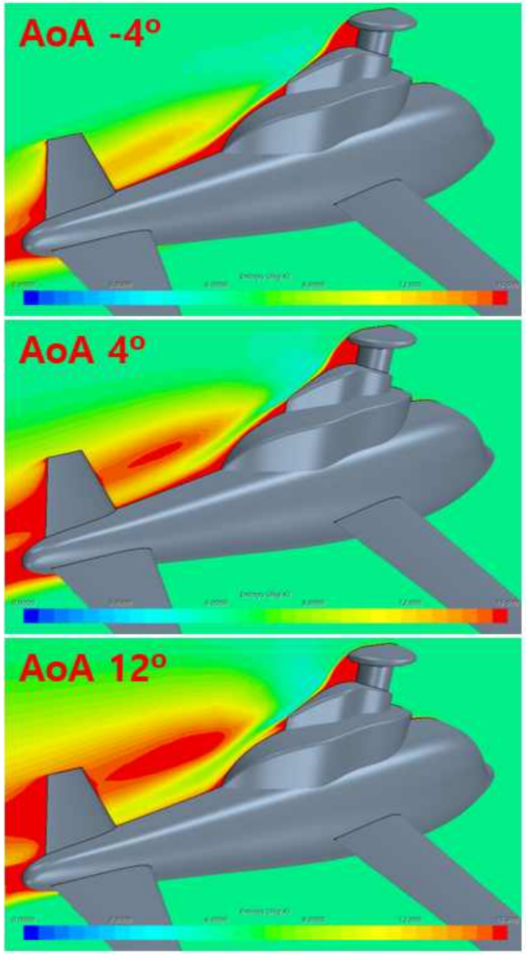

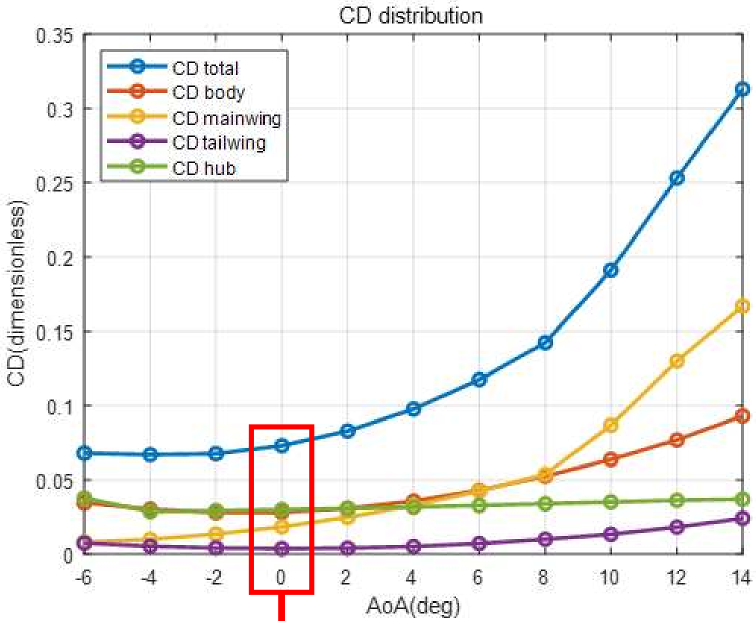

DISTRIBUTION	CL	CL(%)	CD	CD(%)
Total	0.421	100	0.0808	100
Fuselage	0.043	10.22	0.0284	35.15
Main Wing	0.360	85.39	0.0186	23.02
Tail Wing	-0.029	-6.91	0.0038	5.25
Hub	0.047	11.29	0.0300	37.13

- ✓ Remarkably large drag on hub and fuselage
- ✓ Passive Drag Reduction
  - ➢ Extended surface
  - ➢ Extruded groove

Passive Reduction of Fuselage Drag

- Extended Surface on full-scale configuration

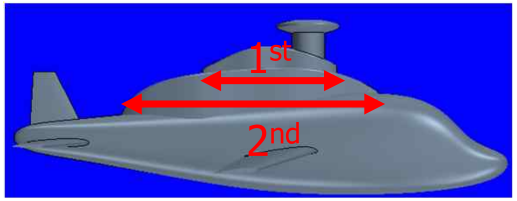

AoA 0°	Original	Extension1	Extension2	Extension3
1st Extension	× 1	× 1.08	× 1.16	× 1.32
2nd Extension	× 1	× 1.1	× 1.2	× 1.3
C_l	0.421813	0.420 (-0.41%)	0.415 (-1.60%)	0.408 (-3.21%)
C_d	0.073120	0.070 (-2.96%)	0.067 (-7.45%)	0.063 (-13.22%)
C_l/C_d	5.768772	5.920 (+2.63%)	6.132 (+6.31%)	6.434 (+11.53%)

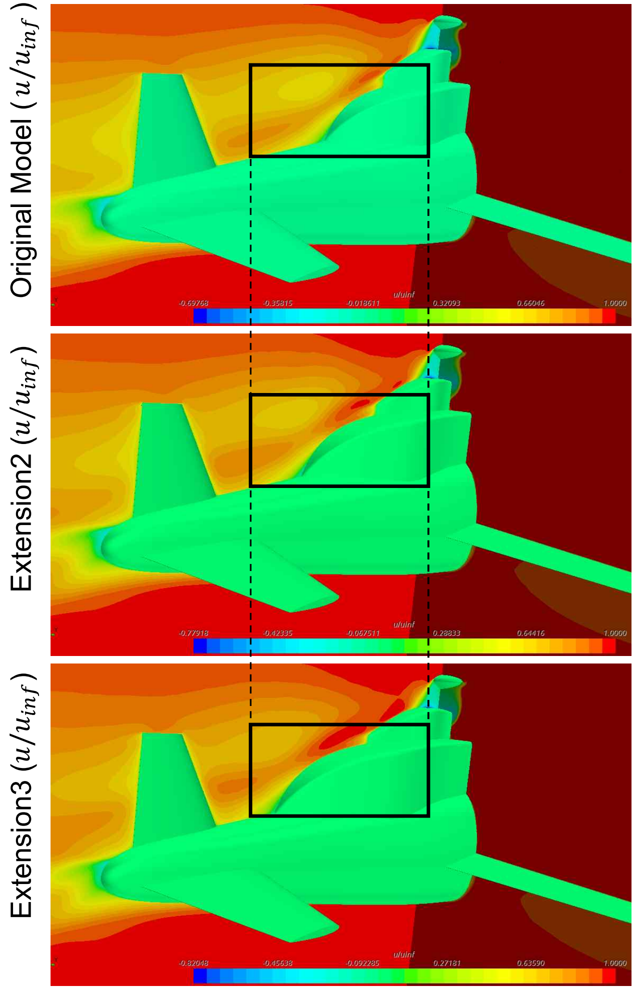

Passive Reduction of Fuselage Drag

- Extruded Groove on Extension 3 Model $(1:1, AoA = 8°, M = 0.3)$

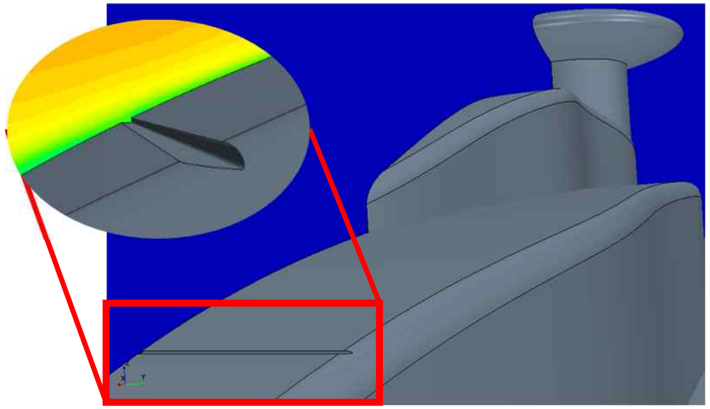

<Applying Extruded Groove at Separation Point>

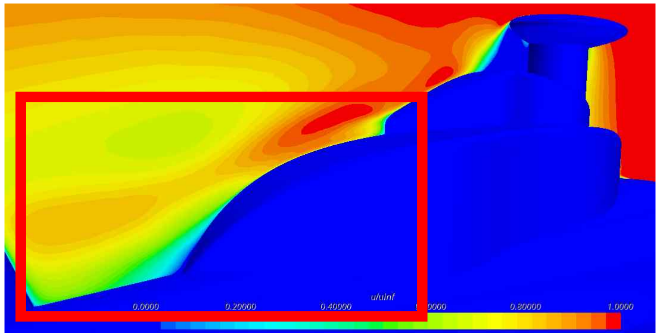

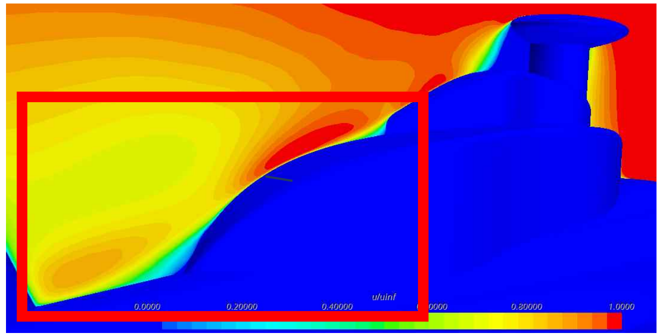

	Extension3	Extension3+Groove
Cl	1.261662	1.23042 (-2.47%)
Cd	0.138796	0.13436 (-3.19%)
Cl/Cd	9.090013	9.157665 (+0.74%)

Active Reduction of Fuselage Drag

Model : ROBIN-mod7

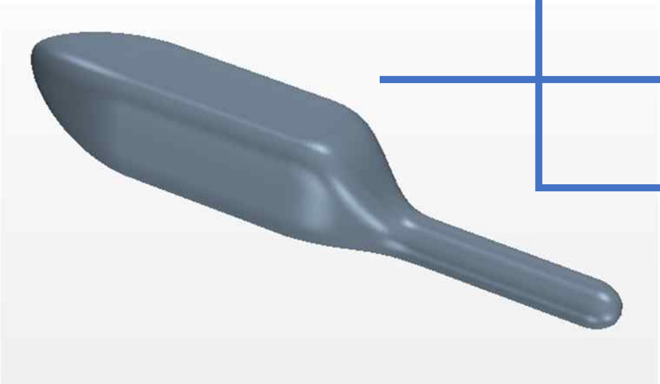

- ✓ **Slot Location**
- ✓ **Injection Angle**
- ✓ **Blowing Momentum**

Schaeffler, Norman W. et al. "Progress towards fuselage drag reduction via active flow control: A combined CFD and experimental effort." (2010).

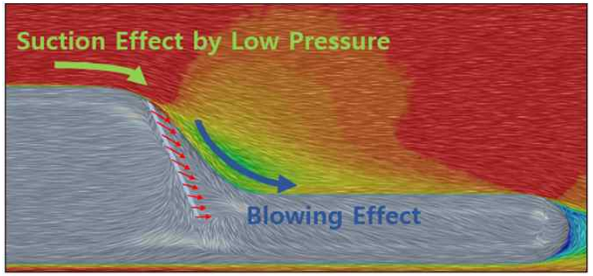

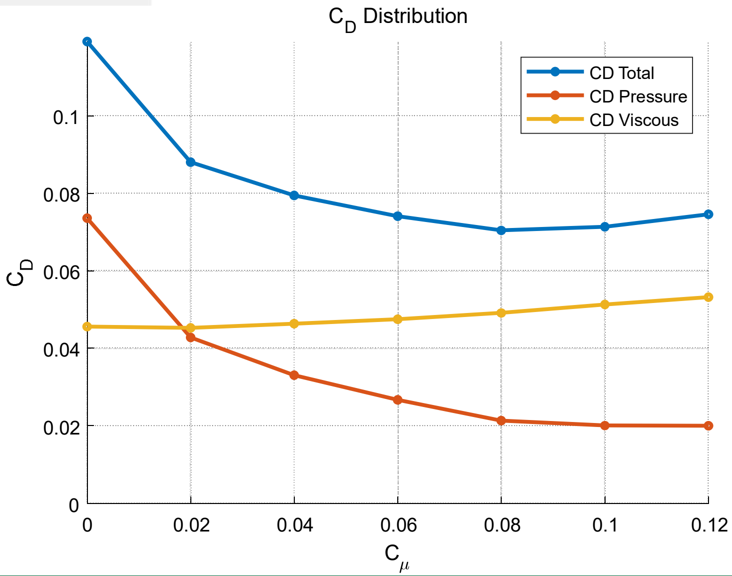

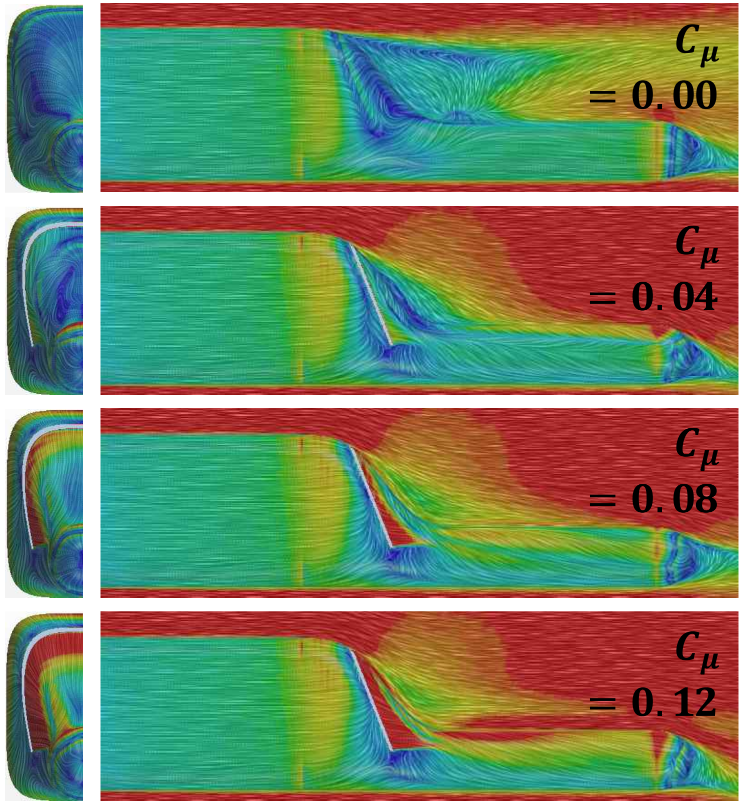

Concluding Remarks

- A hybrid reconstruction method can enhance vorticity-preserving capability of rotorcraft aerodynamics solver.
  - Simulations of PRWIM and HART-II
  - Stacked rotor
  - New approaches : Vorticity confinement and Implicit RK, ….

- Passive and active schemes can reduce the fuselage drag, especially for high-speed compound helicopters.
  - Passive reduction
  - Open loop active reduction
  - Direction : closed loop active control with AI-POD-based controller